

Assembly of Triple-Stranded  $\beta$ -Sheet Peptides at InterfacesHanna Rapaport,<sup>†</sup> Gunter Möller,<sup>‡</sup> Charles M. Knobler,<sup>‡</sup> Torben R. Jensen,<sup>§</sup> Kristian Kjaer,<sup>§</sup> Leslie Leiserowitz,<sup>||</sup> and David A. Tirrell<sup>\*,†</sup>

Division of Chemistry and Chemical Engineering, California Institute of Technology, Pasadena, California 91125,

Department of Chemistry and Biochemistry, University of California, Los Angeles, California 90095,

Materials Research Department, Risø National Laboratory, DK-4000 Roskilde, Denmark, and

Department of Materials and Interfaces, Weizmann Institute of Science, Rehovot 76100, Israel

Received May 2, 2002

Molecular systems composed of peptides or proteins can be programmed to yield intriguing and potentially useful supra-molecular architectures.<sup>1</sup> The surfaces of solid or liquid substrates may induce conformational, orientational, and positional order in molecular assemblies,<sup>2</sup> and peptides composed of alternating hydrophilic and hydrophobic amino acids have been shown by spectroscopic and scanning probe techniques to form  $\beta$ -sheet assemblies at interfaces.<sup>3</sup> Recently, two-dimensional (2D) order in  $\beta$ -sheet monolayers has been demonstrated by grazing incidence X-ray diffraction (GIXD).<sup>4</sup> Long-range order has also been inferred from the preferred orientation of nanocrystals nucleated under  $\beta$ -sheet monolayers at the air–water solution interface.<sup>5</sup> Langmuir films of  $\beta$ -sheet peptides differ from many ordered molecular assemblies<sup>2,6</sup> in that peptide side chains can be engineered to provide scaffolds for further organization of the interface. Here we aimed at generating an ordered 2D molecular assembly composed of triple-stranded amphiphilic peptides arrayed at the air–water interface.

Progress in the design of  $\beta$ -sheet peptides has been based in part on the screening of known protein structures for correlation between sequence and secondary structure.<sup>7</sup> Studies of water-soluble peptides that incorporate  $\beta$ -hairpins (loop regions flanked by two strands interlinked via hydrogen bonds) derived from natural proteins have also contributed to our understanding of the folding and stability of  $\beta$ -sheet peptides.<sup>8</sup> Among the most abundant  $\beta$ -hairpins in natural proteins are the two-residue loops,<sup>9</sup>  $\beta$ -turns of types I' and II', which appear to impose a twist on adjacent peptide strands. In small de novo designed peptides it was shown that the nonnatural amino acid D-Pro at position  $i + 1$  is effective in driving the formation of  $\beta$ -hairpins in aqueous solution.<sup>10,11</sup> L-Pro was found to be almost absent from two-residue  $\beta$ -hairpins of crystalline proteins;<sup>9b</sup> however, in types I and II  $\beta$ -turns L-Pro is the most abundant residue<sup>7b</sup> at position  $i + 1$ . The propensities of L-Pro and D-Pro to promote types I and I'  $\beta$ -turns, respectively, may be rationalized by the match between the dihedral angles  $\phi_{i+1}$  of the turn and the restrained  $\phi$  angles of L-Pro and D-Pro ( $\sim -60^\circ$  and  $\sim +60^\circ$ , respectively).

The 30-residue peptide BS30 was designed to fold into the triple-stranded  $\beta$ -sheet depicted schematically in Figure 1. The proposed architecture depends on formation of two reverse turns, and on registry of the hydrophilic and hydrophobic amino acids along the three strands of the sheet. The main axes of the three amphiphilic strands were anticipated to extend parallel to the plane of the interface in an arrangement that is unlikely to occur in globular proteins, where neighboring strands are twisted relative to one

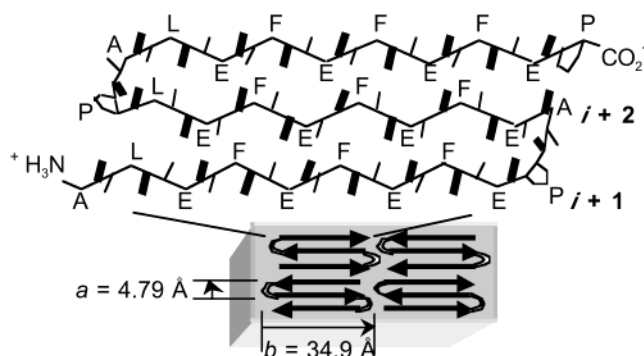


**Figure 1.** Schematic representation of the triple-stranded peptide (top) and possible assembly at the air–water interface (bottom) showing peptide backbone (line), carbonyl, and amine NH groups (thick and thin lines, respectively). Amino acid side chains are designated by the one-letter code; the two amino acids in the turn are designated as the  $i + 1$  and  $i + 2$  residues of a  $\beta$ -hairpin motif. For peptide BS30G (see text) residue  $i + 1$  in each turn is Gly (replacing the L-Pro shown in the scheme).

another.<sup>13</sup> Accordingly, a type II  $\beta$ -turn (which is nearly planar),<sup>9b</sup> has been targeted in the design of BS30, on the assumption that it would better stabilize the parallel orientation of adjacent strands. On the basis of the propensity of L-Pro to occupy position  $i + 1$  of type II  $\beta$ -turns (vide supra), the targeted fold of BS30 places L-Pro at position  $i + 1$  (Figure 1). On the basis of structural studies that have demonstrated that L-Pro-Ala in short peptides assumes the type II  $\beta$ -turn,<sup>14</sup> we chose Ala to occupy position  $i + 2$ . We assumed that the methyl side chain would not destabilize the turn, whether it points into or out of the water subphase. By analogy with our previous design of 2D ordered monolayers of single-stranded  $\beta$ -sheet peptides,<sup>4</sup> Phe and Glu were selected as the alternating hydrophobic and hydrophilic amino acids along the strands. Two Leu residues were placed adjacent to one of the  $\beta$ -turns to provide greater conformational flexibility (compared to that from Phe) and to impose fewer steric restrictions in the region close to the turn. The second peptide studied here, BS30G, is identical to BS30 except that Gly replaces Pro at position  $i + 1$  of each  $\beta$ -hairpin.

Surface pressure versus molecular area isotherms<sup>15</sup> of BS30 indicate a limiting area per molecule ( $\sim 460 \text{ \AA}^2$ ) that corresponds reasonably well to that estimated from the known dimensions of crystalline  $\beta$ -sheet monolayers<sup>4</sup> ( $\sim 16.4 \times 30 = 492 \text{ \AA}^2$ ). The limiting area per molecule is smaller for BS30G ( $\sim 380 \text{ \AA}^2$ ), suggesting either partial dissolution of the peptide in the subphase or coexistence of molecular arrangements that occupy smaller areas at the interface. GIXD and microscopy studies described below support the latter. ATR-FTIR measurements indicate for both peptides the formation of antiparallel  $\beta$ -sheet structure.<sup>15</sup>

\* To whom correspondence should be addressed. E-mail: datirrell@caltech.edu.

<sup>†</sup> California Institute of Technology.

<sup>‡</sup> University of California.

<sup>§</sup> Risø National Laboratory.

<sup>||</sup> Weizmann Institute of Science.

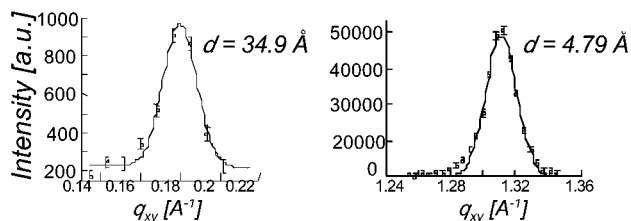


**Figure 2.** Measured GIXD Bragg peaks of BS30 monolayer, corrected for Lorenz-polarization and geometric factors.<sup>15</sup>

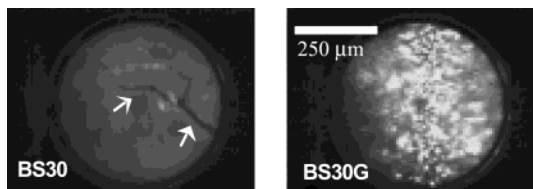


**Figure 3.** BS30 at 500 Å<sup>2</sup>/molecule and BS30G at 250 Å<sup>2</sup>/molecule, at the air–water–interface, imaged by BAM.<sup>15</sup> Arrows mark crack lines in the BS30 monolayer.

GIXD measurements<sup>15</sup> performed on the BS30 monolayer at nominal area per molecule of 500 Å<sup>2</sup>, reveal Bragg peaks at  $q_{xy} = 0.180$  and  $1.311 \text{ \AA}^{-1}$ , corresponding to spacings of 34.9 and 4.79 Å, respectively (Figure 2). The 4.79 Å spacing, characteristic of crystalline  $\beta$ -sheet structures, is generated by peptide strands interlinked by N–H $\cdots$ O=C hydrogen bonds, forming extended hydrogen-bonded ribbons (along  $a$ , Figure 1). The 34.9 Å spacing is attributed to the repeat distance of juxtaposed neighboring hydrogen-bonded ribbons (along  $b$ , Figure 1). The full width at half-maximum,  $\text{fwhm}(q_{xy})$ , of each of the two Bragg peaks yields crystalline coherence lengths<sup>15</sup> along the  $a$  and  $b$  directions of about 250 Å. The  $\text{fwhm}$  of the 4.79 Å Bragg rods<sup>15</sup> corresponds to a film thickness of  $\sim 9$  Å which matches the expected thickness of a monolayer film. On the basis of the relatively low intensity of the 34.9 Å Bragg peak and preliminary X-ray structure factor calculations on a putative 2D lattice (as in Figure 1), we deduce that the BS30 monolayer contains several coexisting packing configurations. BS30 molecules may be packed, for example, by translation along the  $a$  axis through parallel  $\beta$ -sheet hydrogen bonds, in contrast to the proposed packing (by two-fold symmetry about the normal to the water, shown in Figure 1). Such a defect may propagate further disorder in the juxtaposition of neighboring peptide ribbons, by inducing the molecules to be related along the  $b$  direction by translation rather than via two-fold symmetry (shown in Figure 1). Dislocation defects (along the  $b$  direction) may also be the result of the repetitive hydrogen-bonding pattern along the peptide strands. These possible variations in packing would reduce the intensity of the 34.9 Å Bragg peak but would have much a weaker effect on the Bragg peak at 4.79 Å.

BS30G exhibits only a very weak GIXD Bragg peak corresponding to a  $\sim 4.79$  Å spacing, suggesting limited order in the Gly variant of the peptide.

A typical Brewster angle microscopy<sup>16</sup> (BAM) image of a BS30 film, at  $\sim 500$  Å<sup>2</sup>/molecule, visualized directly by reflection, reveals solidlike domains (Figure 3) that span the dimensions of the captured image (0.5 mm in diameter). The solid nature of the domains is evident from their low mobility compared to that from other regions in the film and from the relatively sharp boundaries

and extended crack lines that resemble textures typical of macroscopic solids. The film also contains regions of higher lateral mobility as well as dark regions where presumably molecular density is relatively low.<sup>16</sup> BAM images of BS30G were observed only for the compressed state of the film ( $\sim 250$  Å<sup>2</sup>/molecule) and revealed disordered domains against a dark background. The pronounced differences in reflected intensities indicate regions of variable heights, consistent with the reduced area per molecule observed by surface pressure–area isotherms for BS30G.

This study demonstrates simple design principles for the preparation of ordered macromolecular assemblies at the air–water interface.

**Acknowledgment.** We thank Suzanna Horvath and her staff for peptide synthesis, George Rossman for help in ATR-FTIR, and HASYLAB for synchrotron beamtime. This work was supported by the U.S.–Israel Binational Science Foundation, the U.S. National Science Foundation, the DanSync program of the Danish Natural Science Research Council, and the European Community, TMR-Contract ERBFMGECT950059.

**Supporting Information Available:** Surface pressure–area isotherms, description of GIXD measurements, FTIR spectra, additional BAM images of BS30 (PDF). This material is available free of charge via the Internet at <http://pubs.acs.org>.

## References

- (1) (a) Ghadiri, M. R.; Granja, J. R.; Milligan, R. A.; Duncan, E. M.; Khazanovich, N. *Nature* **1993**, *366*, 324–327. (b) Krejchi, M. T.; Atkins, E. D. T.; Waddon, A. J.; Fournier, M. J.; Mason, T. L.; Tirrell, D. A. *Science* **1994**, *265*, 1427–1432. (c) Choo, D. W.; Schneider, J. P.; Graciani, N. R.; Kelly, J. W. *Macromolecules* **1996**, *29*, 355–366. (d) Fukuto, M.; Heilman, R. K.; Pershan, P. S.; Yu, S. M.; Griffiths, J. A.; Tirrell, D. A. *J. Chem. Phys.* **1999**, *111*, 122–127. (e) Jaworek, T.; Neher, D.; Wegner, G.; Wieringa, R. H.; Schouten, A. J. *Science* **1998**, *279*, 57–60.
- (2) Rapaport, H.; Kuzmenko, I.; Berfeld, M.; Edgar, R.; Popovits-Biro, R.; Weissbuch, I.; Lahav, M.; Leiserowitz, L. *J. Phys. Chem. B* **2000**, *104*, 1399–1428.
- (3) (a) Kaiser, E. T.; Kezdy, F. J. *Proc. Natl. Acad. Sci. U.S.A.* **1983**, *80*, 1137–1143. (b) Osterman, D. G.; Kaiser, E. T. *J. Cell. Biochem.* **1985**, *29*, 57072. (c) DeGrado, W. F.; Lear, J. D. *J. Am. Chem. Soc.* **1985**, *107*, 7684–7689. (d) Xu, G.; Wang, W.; Groves, J. T.; Hecht, M. H. *Proc. Natl. Acad. Sci. U.S.A.* **2001**, *98*, 3652–3657. (e) Powers, E. T.; Yang, S. I.; Lieber, C. M.; Kelly, J. W. *Angew. Chem., Int. Ed. Engl.* **2002**, *41*, 127–130.
- (4) Rapaport, H.; Kjaer, K.; Jensen, T. R.; Leiserowitz, L.; Tirrell, D. A. *J. Am. Chem. Soc.* **2000**, *122*, 12523–12529.
- (5) Bekele, H.; Fendler, J. H.; Kelly, J. W. *J. Am. Chem. Soc.* **1999**, *121*, 7266–7267.
- (6) Ulman, A. In *Organised Molecular Assemblies in the Solid State*; Whitesell, J. K., Ed.; John Wiley and Sons: New York, 1999; pp 1–38.
- (7) (a) Chou, P. Y.; Fasman, G. D. *J. Mol. Biol.* **1977**, *115*, 135–175. (b) Hutchinson, E. G.; Thornton, J. M. *Protein Sci.* **1994**, *3*, 2207–2216.
- (8) For leading references, see: (a) Blanco, F.; Ramirez-Alvarado, M.; Serrano, L. *Curr. Opin. Struct. Biol.* **1998**, *8*, 107–111. (b) Gellman, S. H. *Curr. Opin. Chem. Biol.* **1998**, *2*, 717–725. (c) Lacroix, E.; Kortemme, T.; de la Paz, M.; Serrano, L. *Curr. Opin. Struct. Biol.* **1999**, *9*, 487–493.
- (9) (a) Mattos, C.; Petsko, G. A.; Karplus, M. *J. Mol. Biol.* **1994**, *238*, 733–747. (b) Sibanada, B. L.; Thornton, J. M. *Nature* **1985**, *316*, 170–174.
- (10) (a) Das, C.; Raghobama, S.; Balam, P. *J. Am. Chem. Soc.* **1998**, *120*, 5812–5813. (b) Karle, I.; Awasthi, S.; Balam, P. *Proc. Natl. Acad. Sci. U.S.A.* **1996**, *93*, 8189–8193.
- (11) Stanger, H.; Gellman, S. H. *J. Am. Chem. Soc.* **1998**, *120*, 4236–4237.
- (12) Haque, T. S.; Gellman, S. H. *J. Am. Chem. Soc.* **1997**, *119*, 2303–2304.
- (13) Chou, K. C.; Pottle, M.; Nemethy, G.; Ueda, Y.; Scheraga, H. A. *J. Mol. Biol.* **1982**, *162*, 89–112.
- (14) (a) Aubry, A.; Protas, J.; Boussard, G.; Marraud, M. *Acta Crystallogr., Sect. B* **1977**, *33*, 2399–2406. (b) Prasad, B. V. V.; Balam, H.; Balam, P. *Biopolymers* **1982**, *21*, 1261–1273.
- (15) See Supporting Information
- (16) Fischer, B.; Tsao, M. W.; Ruiz-Garcia, J.; Fischer, T. M.; Schwartz, D. K.; Knobler, C. M. *J. Phys. Chem.* **1994**, *98*, 7430–7435

JA026765J